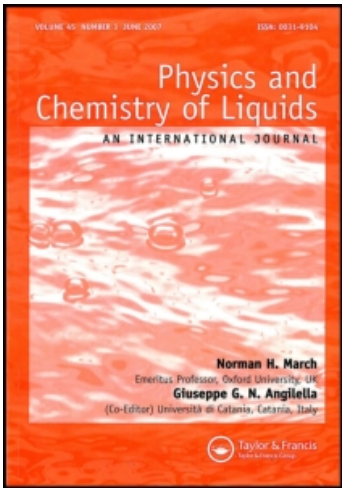

Physics and Chemistry of Liquids

Publication details, including instructions for authors and subscription information:
http://www.informaworld.com/smpp/title~content=t713646857

Clustering of Particles in Colloidal and Molecular Fluids

David M. Heyes[a]
[a] Department of Chemistry, Royal Holloway and Bedford New College, University of London, Surrey, UK

To cite this Article Heyes, David M.(1989) 'Clustering of Particles in Colloidal and Molecular Fluids', Physics and Chemistry of Liquids, 19: 3, 125 — 143
To link to this Article: DOI: 10.1080/00319108908030611
URL: http://dx.doi.org/10.1080/00319108908030611

Phys. Chem. Liq., 1989, Vol. 19, pp. 125-143
Reprints available directly from the publisher
Photocopying permitted by license only

REVIEW ARTICLE
Clustering of Particles in Colloidal and Molecular Fluids

DAVID M. HEYES

Department of Chemistry, Royal Holloway and Bedford New College, University of London, Egham, Surrey TW20 OEX, UK.

(Received 5 October 1988)

A review is given of the nature and implications of cluster formation in colloidal and molecular systems. We consider large clusters that can be described in terms of the fractal dimension and percolation exponents. The role of computer molecular simulation is discussed as a *new* method for probing random clustering of particles, short range structural correlations being of diminished importance here.

KEY WORDS: Fractal, percolation, growth.

1 INTRODUCTION

Randomly associating particles have a complicated non-symmetrical structure and are therefore difficult to characterise. They lack a suitable reference state from which to base perturbation treatments of their properties. (Dense gases have the ideal gas and solids have the Einstein crystal.) This leads one to expect that there may well be an infinite set of parameters needed to characterise their list of properties. This is a somewhat depressing concept and progress would otherwise have been slow but for a major advance made about 10 years ago. Mandelbrot then introduced the concept of *fractal* objects which allowed the properties of these cluster forming particles to be encapsulated in a quantitative fashion using a small number of parameters called fractal dimensions[1]. Since then it has become apparent that far from being the exception, *fractal aggregates* are so common in nature that they surely must now have an importance at least equal to that of the crystal, liquid and gaseous phases of matter[2,3]. They are, for example, the automatic outcome of the natural "growth" processes involved in sedimentation, deposition and flocculation.

A fractal object has a mass, $m(r)$, that scales as its 'effective' radius, r, as

$$m(r) \sim r^{d_f}, \tag{1}$$

where d_f is the fractal dimension. The value of $d_f \leq d$, where d is the dimension of the space in which the fractal exists. As the object becomes more 'open' then it will have a smaller fractal dimension.

Although non-equilibrium growth processes are a common source of fractals they also occur in equilibrium particle distributions, for example. The long-range structure of molecular fluids at arbitrary density can also be described by fractals. The different

routes have an influence on the value of d_f, which is therefore a probe of the underlying physics.

2 COLLOIDAL AGGREGATES

Irreversible clustering is of predominant interest here. The aggregation of stabilised particles ('monomers') suspended in a liquid can be induced by the addition of a salt solution for charge-stabilised particles and other (smaller) particles for sterically stabilised particles. In the case of charge stabilisation, the salt solution decreases the Debye–Hückel screening length so that particles can approach close enough for the van der Waals interactions to 'trap' the particles in a pair-potential well. The monomer size and salt concentration can be manipulated to cause the growth of macroscopic clusters (~ 1 mm) within an experimentally suitable time-scale.

The properties of the aggregates can often be expressed in terms of a fractal dimension, although the value of d_f is often sensitive to the particular property.

The structures obtained have a density-density correlation function, $g(r)$ of the power law form, $g(r) \sim r^{d_f - d}$.[4] This structure can be probed by low-angle scattering of neutrons, X-rays or visible light. The scattered intensity with scattering angle Θ is given by, $S(k) \sim k^{-d_f}$, where $k = 4\pi \sin \Theta/\lambda$ and λ is the wavelength of the incident beam[2]. The structure factor obeys this relationship for $r_0 \ll k^{-1} \ll R$, where r_0 is the radius of the monomer and R is the approximate radius of the cluster. In the zero k limit, $(S(k) - S(0))/S(0) \sim k^2R^2$. Therefore, scattering experiments can lead to some very useful geometrical and size parameters for the clusters[5].

Lattice simulations of idealised aggregation mechanisms have been made, which have helped interpret the experimental data[6]. The growth of a cluster could be viewed as the accumulation of randomly walking monomer units attaching themselves to a single growing cluster. Despite recent observations of some dependence on the lattice symmetry, this diffusion-limited-aggregation or *DLA* model leads to a reproducible $d_f = 1.70$ in $2d$ and $d_f = 2.50$ in $3d$. (Asymptotically large *DLA* clusters grown in $2d$ on lattices with m-fold symmetry exhibit m-fold star-shaped anisotropy[7].) The cluster-cluster aggregation or *CCA* model is an alternative *scenario*. Here, the larger clusters grow by the coming together of smaller clusters. This leads to more open clusters, characterised by $d_f = 1.44$ in $2d$ and $d_f = 1.78$ in $3d$. Some recent studies on gold and silica particle dispersions, and polystyrene lattices[8] of $r_0 \sim 7 - 500nm$ have yielded d_f of 1.75 ± 0.1 when fast aggregation is induced by high concentration of an inert smaller particle (an osmotic effect called 'depletion' flocculation[9])[10] or salt solution[8]. This conforms to the *CCA* model. Slow aggregation yields $d_f = 2.1 \pm 0.1$[4,5,11].

In the fast aggregation regime there is a power-law increase with time of the cluster size $r \sim t^{1/d_f}$.[8] Power law relaxation is a signature of critical slowing down, observed in e.g., glass-formation[12]. The time-dependence of the growth can also be of a stretched exponential form, $\exp -(t/\tau)^{\beta}$ or the algebraic form $\sim t^{-\alpha}$ depending on the nature of the microscopic dynamics e.g., the distribution of energy barriers for deposition. The fractal clusters grown are kinetically unstable. Fast aggregating

particles have been observed to restructure with time to a more compact structure with $d_f = 2.1 \pm 0.1$.

As will be discussed below the physical properties of the aggregates are often dominated by the largest cluster. When this cluster extends to infinite extent it is said to "percolate". Percolation theory has enabled the structural statistics of an ensemble of clusters to be encapsulated in a number of scaling laws of the form, $X \sim \varepsilon^p$ where X is some statistical property and ε is the "distance" from the density at which percolation takes place (the so-called "percolation threshold")[13-14]. The exponent p is universal, i.e., is independent of lattice symmetry and the nature of the interactions (but does depend on the dimension). So far, their are less than 10 exponents that specify the entire structural and geometrical statistics of the lattice system. Physical properties also appear to depend on similar relationships, although here the link is somewhat less well-founded. This is because the (imprecise) distance-scale of the intermolecular forces governing the physical property has to map onto the geometry of the percolation clusters. Despite this reservation, the approach has had great success. For example electrical conductivity of conducting particles in an insulating medium goes as $\sim\varepsilon^t$, where $t = 1.27$ in $2d$ and $t = 1.9 \pm 0.1$ in $3d$[15]. The elasticity of the fractal networks was at first thought to be proportional to the electrical conductivity of the corresponding random resistor network. It is now established that the elasticity approaches zero at the percolation threshold with an exponent, T, much larger than t. T is 3.9 ± 0.3 in $2d$[16]. The value of T in $3d$ would appear to be close to 4.0 also[17]. It has been proposed that, $T = t + 2\nu$, where ν is a percolation statistics exponent (see below)[18]. The threshold density, for rigidity percolation coincides with the percolation threshold for strongly associating aggregates but occurs at higher density for weaker interacting particles (because the infinite cluster back-bone needs to be more multiply interconnected)[19,20]. One step further removed from this is a break-down stress in strained lattices[21] and yield-stress in aggregates[17]. Preliminary studies indicate similar scaling laws also.

3 MOLECULAR FLUIDS

We now consider clusters of molecular fluids and some of the principles that determine their formation, in terms of Percolation statistics. For this we need to specify our meaning of a cluster. A cluster is defined as a group of molecules interconnected by an arbitrary coordination-distance. In an infinite system above the percolation threshold number density there is a finite probability that clusters will form spanning all space. There are universal exponents that characterise cluster statistics *about* the percolation threshold in lattice systems composed of non-interacting particles[13,14]. In lattice systems universality refers to the independence of the value of the exponents to lattice coordination number. In calculations on *off-lattice or continuum* noninteracting disks[22] and spheres[23] the exponents are the same as those from the lattice simulations. Recent studies on continuum interacting fluids generated by Monte Carlo simulation suggests that the values of these exponents are the same for these assemblies, as well as being independent of the nature and range of

the interaction potential. The fluids studied so far by MC simulation have been hard-spheres[24], square-wells[25] and adhesive-spheres[26].

In continuum systems, a set of particles is considered to be part of the same cluster if each member is separated from at least one of the others by a distance $\leq \sigma_s$, which is arbitrary but is usually $\sim\sigma$, the core diameter of the particle. A percolating cluster is a special cluster having infinite extent. Within the framework of the periodically repeating cells of Molecular Dynamics, a sufficient criterion for percolation is for a particle and its image to belong to the same cluster. Of particular interest is the ratio, σ_s/σ and its influence on the exponents. As this ratio diminishes to unity the hard-core starts to dominate the extent of overlap of the shells. We term this the soft-core to hard-core transition.

To maintain consistency with accepted notation, the density is given the symbol, p, here, rather than, ρ, as is usual for the reduced density of continuum fluids treated in molecular simulation. For an infinite number of molecules there is a well-defined density, p_c, at which there is a finite probability of finding a percolating cluster[13,14]. Above and below the percolation density many finite sized clusters exist. These occupy the holes in the percolating cluster above p_c. The distribution of different sized clusters is characterised by the cluster number distribution function, n_s, which is the time average number of clusters containing s particles, N_s divided by N i.e., $n_s = N_s/N$. This is consistent with the definition used in other continuum works[23,27], whereas the cluster number definition used in lattice studies is pN_s/N[13,14]. For finite periodic systems there is an upper bound on s, i.e., $1 \leq s \leq N$.

The behaviour of lattice systems *close to* p_c is described in terms of the following critical exponents.

The following summations involving n_s will only involve non-percolating clusters. Let $\xi(p)$ be the "correlation" lengthscale of the largest cluster, then[13,14],

$$\xi(p) \propto |p - p_c|^{-\nu}. \tag{2}$$

In $1d$, $\nu = 1$, in $2d$, $\nu = 1.35$ and in $3d$, $\nu = 0.88 \pm 0.02$[13]. Therefore ξ diverges at p_c, approaching from either side, which is typical of critical behaviour. The zero'th moment of n_s is,

$$\Omega = \sum_s p(n_s(p) - n_s(p_c)) \propto |p - p_c|^{2-\alpha}. \tag{3}$$

In $1d$, $\alpha = 1$, in $2d$, $\alpha = -0.67$ whereas in $3d$ the value is not known[3]. Here and for all the sums below we are interested in the "single" or nonanalytic part of the sum over all cluster sizes[13]. For each sum we must subtract off the analytic background. This is so we isolate that part of the sum dominated by the representative (i.e., largest) cluster in the vicinity of the percolation threshold. Let the percolation probability, P_∞, be the fraction of molecules found in the percolating cluster. Then[14,26],

$$P_\infty \propto (p - p_c)^\beta. \tag{4}$$

where in $1d$, $\beta = 0$, in $2d$, $\beta = 0.14$ and in $3d$, $\beta = 0.454 \pm 0.008$[13] and $p \geq p_c$. In lattice studies this corresponds to the fraction of occupied sites belonging to the infinite

percolating network. The susceptibility, χ, is

$$\chi = \sum_s{}' s^2 n_s(p) \propto |p - p_c|^{-\gamma}. \tag{5}$$

where in $1d$, $\gamma = 1$, in $2d$, $\gamma = 2.43$ and in $3d$, $\gamma = 1.78 \pm 0.06$[6]. The "′" denotes the omission of the largest cluster at each sample configuration. The largest cluster discovered each time step can either be a percolating cluster, should one (or more) exist, or the largest non-percolating cluster (should there not be a percolating cluster). In polymer science the *susceptibility*, χ, corrresponds to the *mass average molecular mass* whereas $\sum_s' sn_s(p)$ corresponds to the *number average molecular mass*. About p_c,

$$\chi = c_- |p - p_c|^{-\gamma}, \tag{6}$$

for $p \leq p_c$ and,

$$\chi = c_+ |p - p_c|^{-\gamma}, \tag{7}$$

for $p \geq p_c$. The amplitude ratio, c_-/c_+ is different for lattice (≈ 10) and continuum systems (≈ 2)[28] in $3d$. For both ensembles the clusters are larger below p_c than above p_c for the same $|p - p_c|$. The different amplitude ratios suggest that the percolating clusters are more open in continuum than in lattice assemblies[28]. Although the susceptibility exponent, γ is universal the corresponding amplitude ratio does depend on the nature of the intermolecular interactions and the nature of the space (whether discrete or continuous).

The functions Ω, P_∞ and χ require finite-scaling corrections for these small periodic systems.

The *finite-scaling hypothesis* supposes that physical properties are homogeneous functions of the critical-coupling parameters, $\varepsilon = |(p - p_c(L))/p_c(L)|$ and the length-scale of the system, L. Recall that, if $f(x, y)$ is a homogeneous function of two variables it obeys the following for an arbitrary constant, λ,

$$f(x, y) = \lambda^c f(\lambda^a x, \lambda^b y), \tag{8}$$

e.g., if $f(x, y) = x^2 y^3$, then $c = -2a - 3b$. By choosing $\lambda^b = y^{-1}$ then $f(x, y)$ can be written as,

$$f(x, y) = y^{-c/b} f(y^{-a/b} x, 1). \tag{9}$$

Returning to two cluster averages discussed in the text, $P_\infty = f(\varepsilon, L)$ and $\chi = g(\varepsilon, L)$ can be written in the homogeneous forms,

$$P_\infty = L^{-\beta/\nu} f(L^{1/\nu}\varepsilon, 1) \tag{10}$$

where $c = \beta$, $a = -1$ and $b = \nu$, and

$$\chi = L^{\gamma/\nu} g(L^{1/\nu}\varepsilon, 1). \tag{11}$$

where the quantity $L^{1/\nu}\varepsilon \propto (L/\xi)^{1/\nu}$ is therefore essentially a ratio of two length-scales. In the limit, $L \to \infty$ and $\xi \ll L$ then $P_\infty \sim \varepsilon^\beta$ and $\chi \sim \varepsilon^{-\gamma}$. This indicates that $f(L^{1/\nu}, 1) \to (L^{1/\nu}\varepsilon)^\beta$ and $g(L^{1/\nu}\varepsilon, 1) \to (L^{1/\nu}\varepsilon)^{-\gamma}$ in this limit. In the other limit, $L^{1/\nu}\varepsilon \to 0$, $\xi \gg L$ then f and g must reduce to L dependent constants.

There is another universal function,

$$\Theta = \sum_s (sn_s(p_c) - sn_s(p))e^{-hs} \propto h^{1/\delta}, \tag{12}$$

where h is a dummy variable and in $1d$ $\delta = \infty$ in $2d$, $\delta = 18$ and in $3d$, $\delta = 5.0 \pm 0.5$ in 3D[14]. At the percolation threshold[14],

$$n_s(p_c) \propto s^{-\tau}. \tag{13}$$

$$n_s(p) = n_s(p_c)f(z),\ z \equiv (p - p_c)s^{\sigma};\ s \to \infty,\ p \to p_c. \tag{14}$$

where $f(z)$ is a universal function. In random lattice percolation the critical exponents are interrelated by scaling laws,

$$\tau = 2 + 1/\delta,\ \sigma = 1/(\nu + \beta),\ 2 - \alpha = \gamma + 2\beta = \beta(\delta + 1) = d\nu, \tag{15}$$

where d is again the dimension of the space[13,14,29].

To illustrate these scaling laws, we show some preliminary results of $2d$ Lennard-Jones fluids, using the Molecular Dynamics, MD, method[30–32]. These recent continuum simulations have shown that only certain of the percolation exponents are readily obtained from the small systems considered by microscopic computer simulation. Those requiring information above the percolation threshold are not obtainable because of finite N artefacts. However, we can readily obtain τ, d_f and to a somewhat lesser degree of accuracy ν. The details of the MD technique used for particles interacting via the LJ potential,

$$\phi(r) = 4\varepsilon((\sigma/r)^{12} - (\sigma/r)^6), \tag{16}$$

have been described elsewhere[9]. The MD simulations were performed on $2d$ and $3d$ systems. In $2d$, square unit cells of area A were used containing N = 50,450 and 1250 particles. In $3d$ systems up to $N = 864$ were considered. The Verlet algorithm was used to increment the positions of the molecules. LJ reduced units were used throughout, i.e., $k_B T/\varepsilon \to T$, and number density, $\rho = N\sigma^2/A$. Distance is in LJ σ.

The cluster-search routine selects the percolating clusters that span all (periodic) space, not *just* those that span the MD cell[30].

The percolation threshold density in the thermodynamic limit (i.e., $N \to \infty$) can in principle be estimated from finite-N calculations by extrapolation. We make use of the density at which the probability of discovering a percolating cluster in a time step—the percolation fraction, P—equals 0.5[26]. This is because the density at which $P = 0.5$ shows the least system size dependence, as shown in Figure 1, for a $3d$ system. The $P(p)$ curves become sharper increasing N and with decreasing p_c but all have the same rounded appearance. Finite scaling gives[26],

$$p_c(N \to \infty) = p_c(N) - aL^{-1/\nu}. \tag{17}$$

where L is the sidelength of the MD cell ($L = (N/\rho)^{1/3}$) and a is a constant depending on σ_s and T. It is extremely difficult with the range of system sizes (i.e., N) and available computer time to obtain an accurate estimate of ν by this route. The percolation fraction is not an intensive quantity so the statistics are not improved by using large systems. Indeed, they decrease because the number of time steps that can be consumed decreases as N increases.

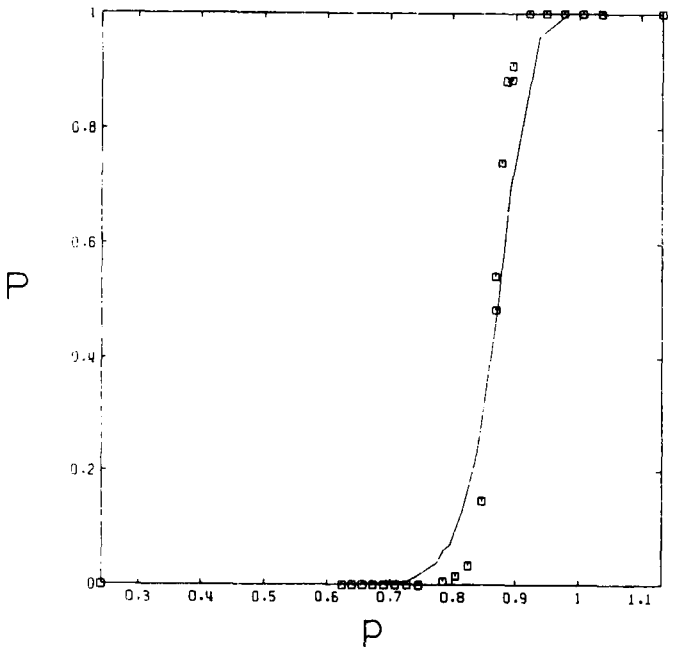

Figure 1 The percolation fraction, P, against density, p in $3d$ for $T = 1.4562$, $\sigma_s = 1.02816$. *key*: $N = 108$ (line) and $N = 864$ (squares). Note the small shift of $P = 0.5$ to lower p for increasing N, in line with scaling arguments.

Percolation theory cannot predict the value of p_c. The continuum wotk to data on p_c has been performed on hard-core particles and has revealed some interesting trends. Bug *et al.*[25] found that attractive interactions can either lower or raise p_c, depending on the value of the width of the potential well, and the value of σ_s/σ. They found that in the hard-core limit the percolation density decreases as temperature descends to the critical temperature, T_c. This is because the attractive interations induce 'extra' local connectivity. In contrast, in the soft-core limit, p_c, increases sharply in the vicinity of the liquid-vapour coexistence line. This is because the attractive interactions contract the local structure at low density so that these 'blobs' find it more difficult to connect together over long distance scales. LJ simulations on $2d$ and $3d$ systems reveal that the attractive interactions also affect p_c. However, the form differs from the previous square-well potential results. In the hard-core limit, p_c, increases slightly as T drops to T_c. This we suggest is due to a contraction of the cage of particles around each particle, inhibiting long range connectivity. In the soft-core limit, the opposite trend is observed. This we ascribe to the enhanced connectivity due to the attractive interactions. It is not yet known why the T dependence of p_c should be opposite for square-well and Lennard-Jones fluids. Both situations are intuitively plausible and could be affected by the *shape* of the interaction potential as well as the well-depth. Figure 2 illustrates the $2d$ LJ display of particles for $\sigma_s/\sigma = 1.2$ and 0.9.

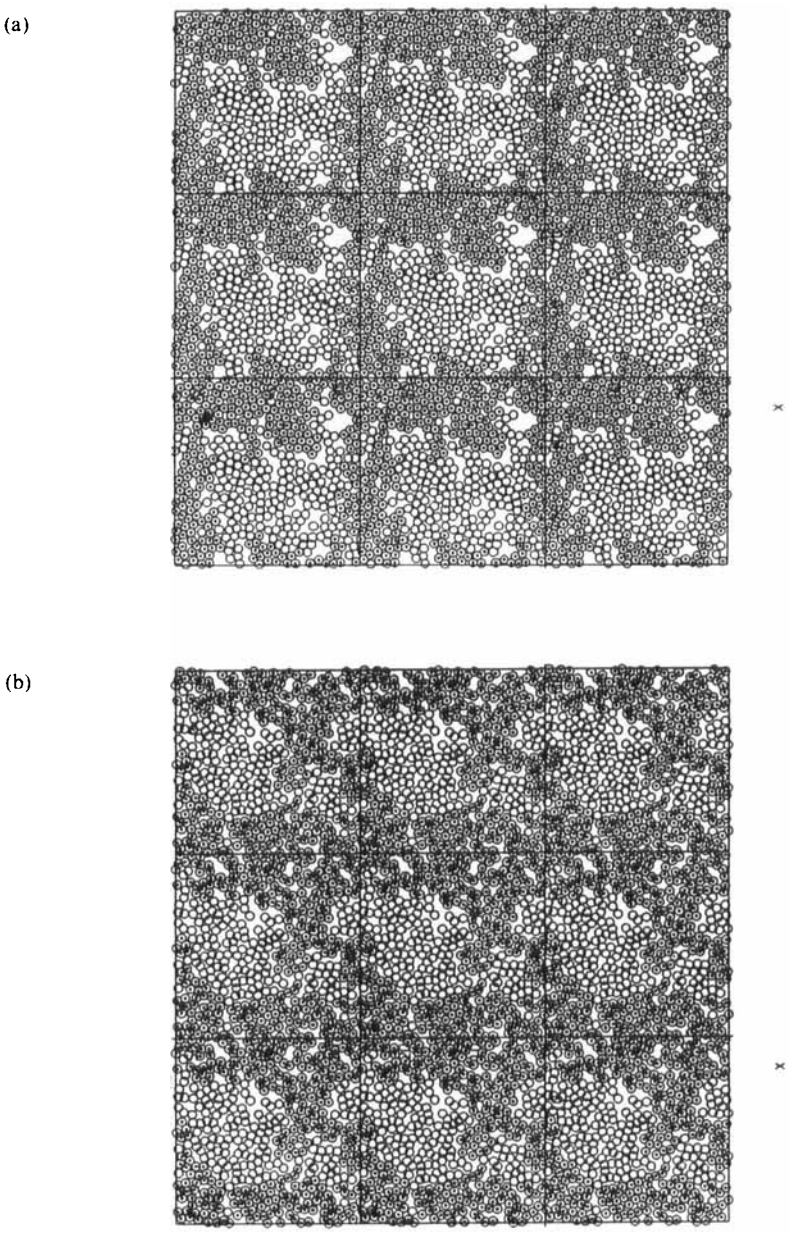

Figure 2 Examples of non-percolating and percolating clusters in two-dimensional periodically repeating cells. 9 ($2d$) MD cells are shown. The large circles (diameter = σ_s) containing smaller circles at their centres form part of the percolating backbone. The circles with no centred inner circles form part of the included (non-percolating) clusters. The central square is the real MD cell, the surrounding cells are its images. Key, (a) $p_c = 0.63240$, $T = 0.6$, $\sigma_s = 1.2$ and $N = 450$; (b) $p_c = 0.662378$, $T = 10.0$, $\sigma_s = 1.2$ and $N = 450$.

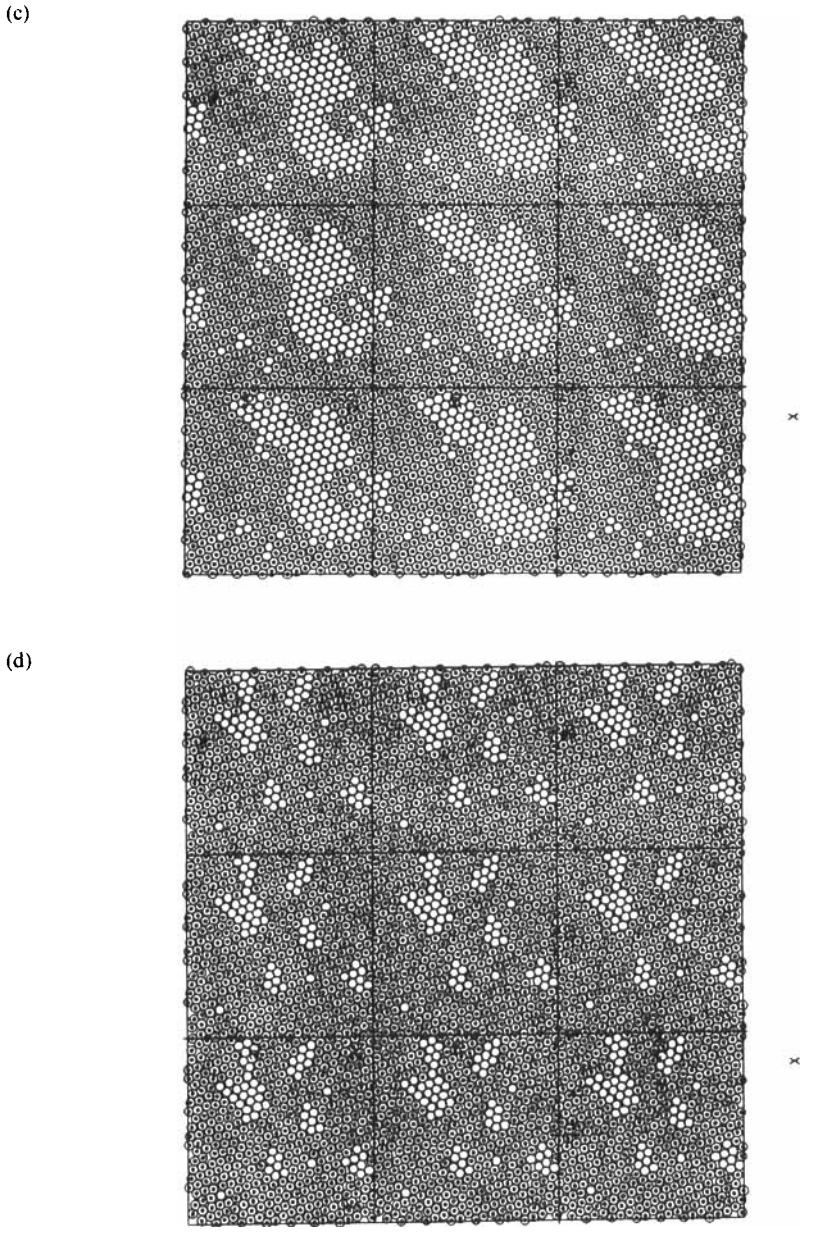

Figure 2 (*continued*) Examples of non-percolating and percolating clusters in two-dimensional periodically repeating cells. 9 (2*d*) MD cells are shown. The large circles (diameter = σ_s) containing smaller circles at their centres form part of the percolating backbone. The circles with no centred inner circles form part of the included (non-percolating) clusters. The central square is the real MD cell, the surrounding cells are its images. Key, (c) $p_c = 1.398381$, $T = 0.6$, $\sigma_s = 0.9$ and $N = 450$; (*d*) $p_c = 1.344638$, $T = 10.0$, $\sigma_s = 0.9$ and $N = 450$.

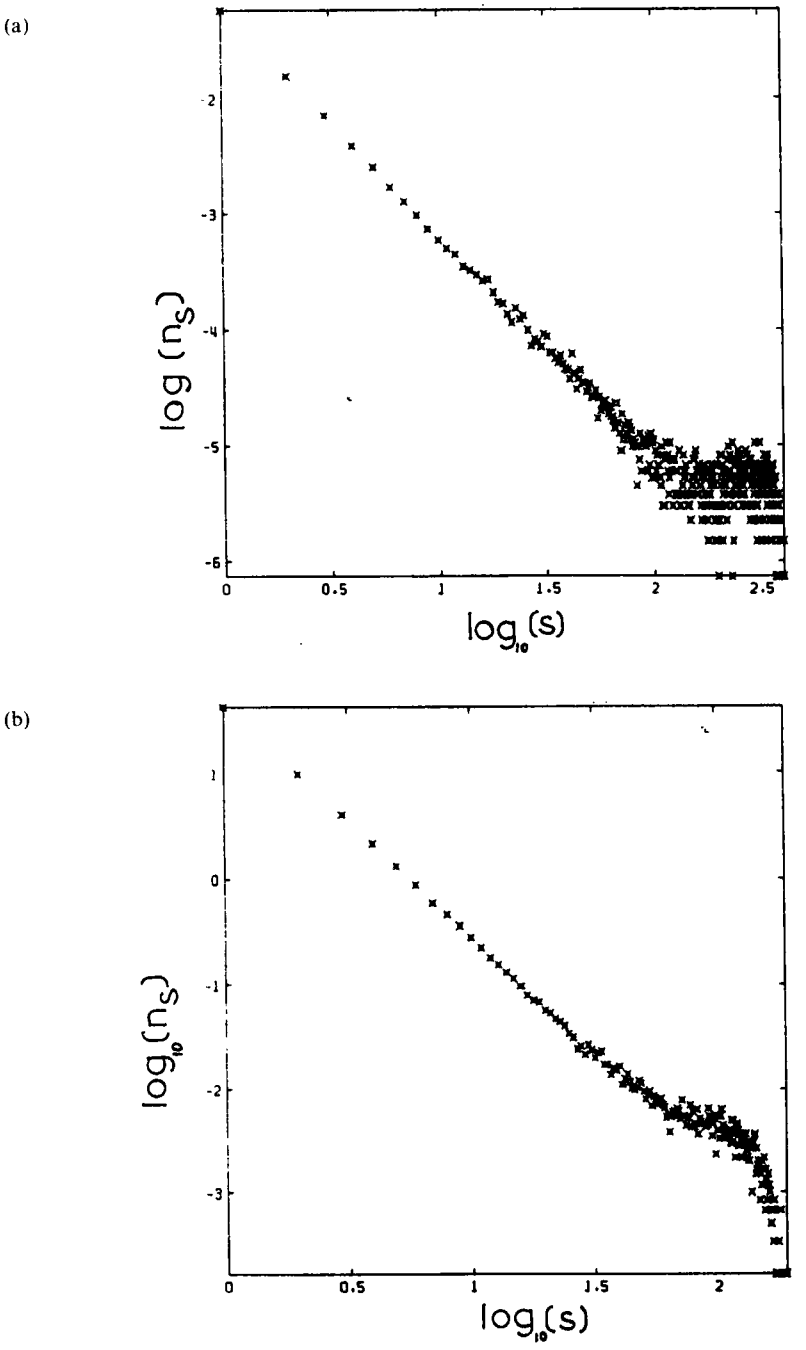

Figure 3 The cluster number distribution for non-percolating clusters, $n_s(s)$ for the p_c LJ state points, (a) $p_c = 1.010848$, $T = 5.0$, $\sigma_S = 1.0$, $N = 450$, $\tau = 2.0 \pm 0.1$ and $2d$, (b) $p_c = 1.2564$, $T = 6.0$, $\sigma_S = 0.9226$, $N = 256$, $\tau = 2.15 \pm 0.1$ and $3d$.

(c)

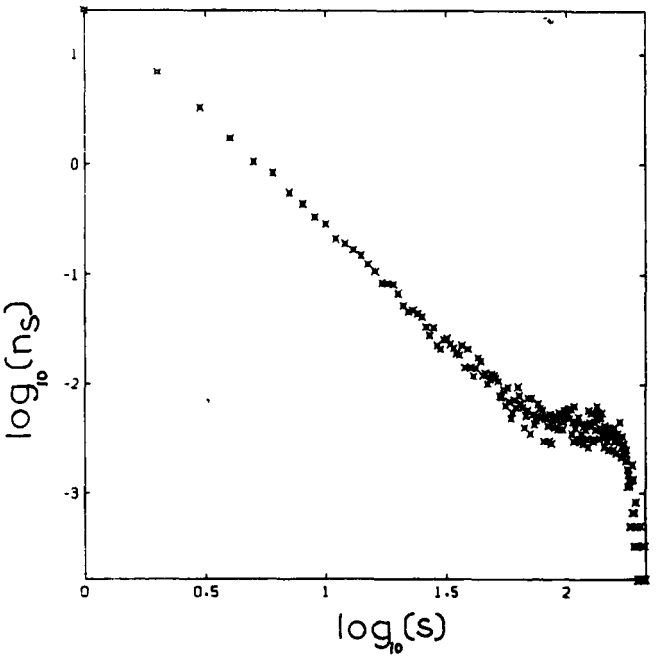

Figure 3 (*continued*) The cluster number distribution for non-percolating clusters, $n_s(s)$ for the p_c LJ state points, (c) $p = 0.260933$, $T = 6.0$, $\sigma_S = 1.31751$, $N = 256$, $\tau = 2.13 \pm 0.1$, and 3*d*.

In 3*D* the LJ percolation threshold for a wide range of state points has been studied. Four (T, σ_s) values have been considered in detail, each with a range of p about p_c, two in the hard-core limit and two going towards the soft-core limit, at $\sigma_s/\sigma_{HS} = 1.05$ and 1.5, respectively. We have taken an effective temperature dependent hard-core diameter[32]. In the hard-core limit $T = 1.4562$, $\sigma_s = 1.02816$ and $T = 6.0$, $\sigma_s = 0.92226$. In the soft-core limit $T = 1.4562$, $\sigma_s = 1.4688$ and $T = 6.0$, $\sigma_s = 1.31751$. The cluster statistics on both sides of the percolation transition were monitored for a range of system sizes. In the hard-core limit $T = 1.4562$, $\sigma_s = 1.02816$ and $T = 6.0$, $\sigma_s = 0.92226$, the p_c are 0.868 ± 0.001 and 1.253 ± 0.001, respectively. In the soft-core limit $T = 1.4562$, $\sigma_s = 1.4688$ and $T = 6.0$, $\sigma_s = 1.31751$, the p_c are 0.164 ± 0.001 and 0.260 ± 0.001, respectively.

When a PC is observed that is a *ca.* 1 % probability that two PC will be observed at the same time for $P \approx 0.5 \pm 0.3$. This is independent of T or σ_s. In contrast, as $P \to 1$ or $P \to 0$ two percolating clusters are never observed simultaneously. This trend can be rationalised as follows. At low p any incipient percolating cluster is tenuous, a break anywhere will not form two percolating clusters because the two halves will not exceed the critical size needed to percolate. As $P \to 1$ the percolating cluster is highly branched and interconnected. Therefore although the two clusters of a PC separated in half would exceed the critical size needed to percolate, the probability of breaking all the bonds needed to form these two clusters would be vanishingly small.

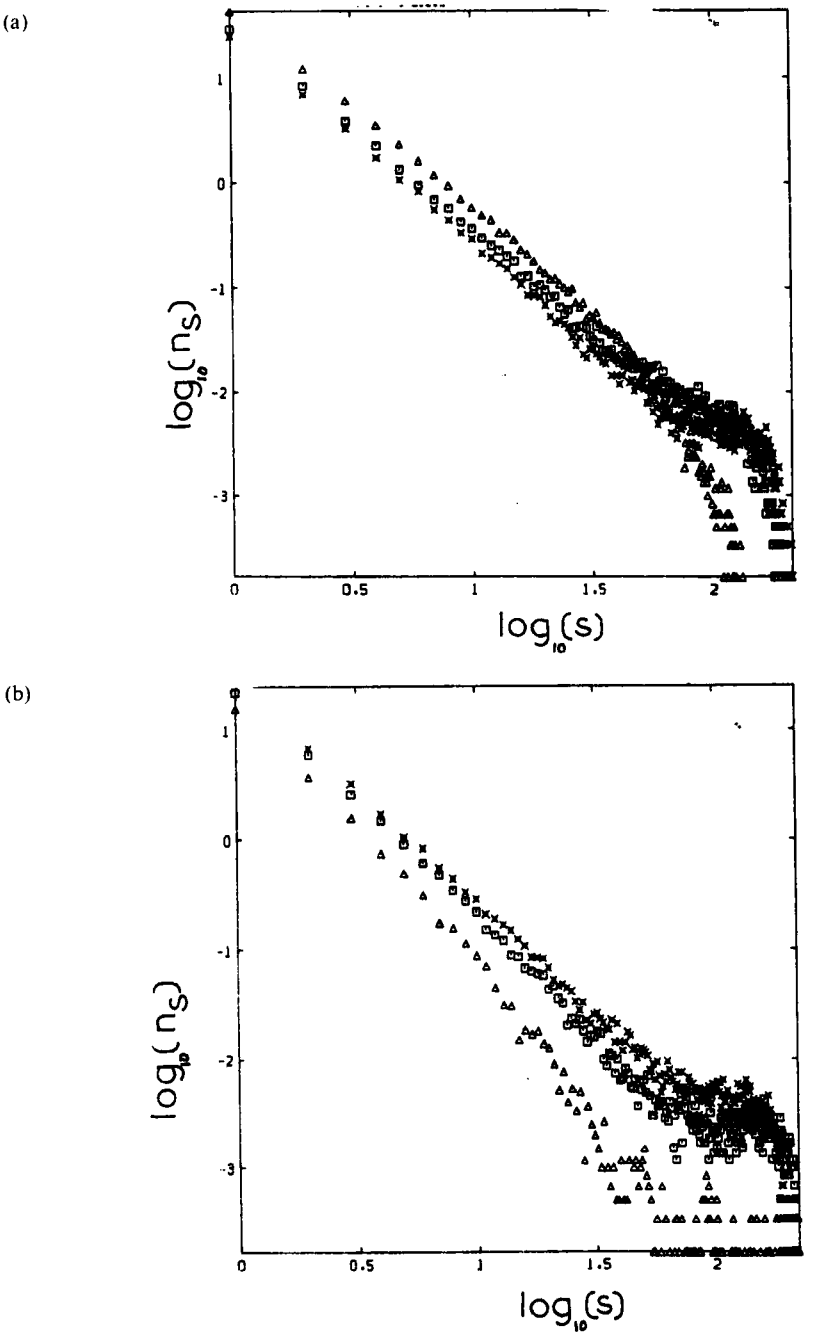

Figure 4 The $n_s(s)$ for the state points: (a) $p_c = 0.26093$ (×), $p = 0.24787$, (square), $p = 0.212517$ (△) $T = 6.0$, $\sigma_s = 1.3175$, $3d$ and $N = 256$; (b) $p_c = 0.26093$ (×), $p = 0.273976$, (square), $p = 0.302059$ (△) $T = 6.0$, $\sigma_s = 1.3175$, $3d$ and $N = 256$.

(c)

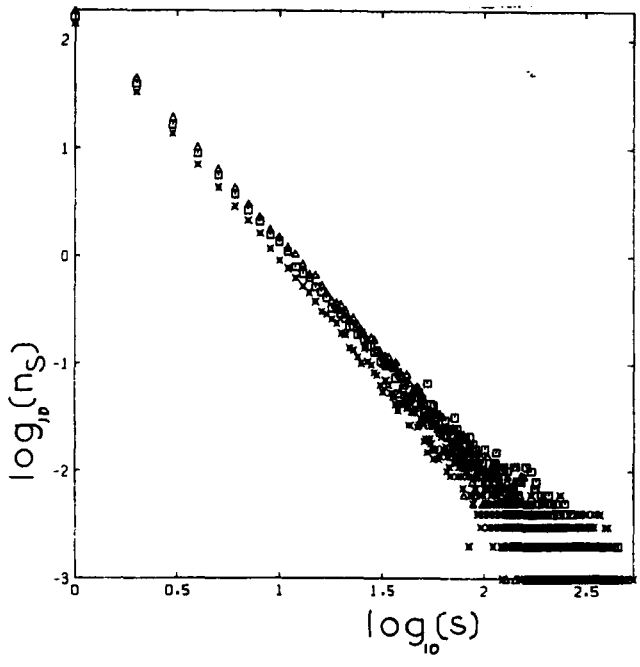

Figure 4 (*continued*) The $n_s(s)$ for the state points: (c) $p_c = 0.86821$ (×), $p = 0.846505$, (square), $p = 0.825342$ (△) $T = 1.4562$, $\sigma_s = 1.02816$, $3d$ and $N = 864$.

At the percolation threshold, lattice and previous continuum work suggest the following simple power law dependence,

$$n_s(p_c) = As^{-\tau}. \tag{18}$$

Lattice percolation gives $\tau = 2.0$ in $2d$ and $\tau = 2.2$ in $3d$[13,14]. Figure 3 shows some typical examples that, within statistical uncertainty, agree with these values for τ. Interestingly, this dependence applies from $s = 1$, which is not the case in lattice studies. One could argue that lattice models are "physically" unrealistic in the small s regime because of discrete coordination numbers.

We now consider the cluster number distribution function, n_s, above and below p_c. Figure 4 gives typical examples. As is revealed there, the $n_s(p)$ in the vicinity of p_c are very similar in form to $n_s(p_c)$, manifesting a change in the prefactor A only. Removed from p_c, random lattice percolation suggests, $n_s(p) = n_s(p_c)f(z)$, $z \equiv (p - p_c)s^{\sigma}$[14]. The form of $f(z)$ is such that descending just below p_c, $n_s(s)$ increases for small s but decreases for large s. As $p - p_c$ becomes more negative then this change in behaviour moves progressively to smaller s. This is consistent with the observation that the maximum size of a non-percolating cluster occurs *just below* p_c. As the total number of non-percolating clusters increase progressively below p_c this observation indicates that, at least close to p_c, the number of small clusters grows at the expense of the larger ones.

Above p_c the change in $n_s(p)$ from $n_s(p_c)$ is quite different. There are always fewer clusters of all sizes s than at p_c, a trend which becomes more pronounced as $p - p_c$

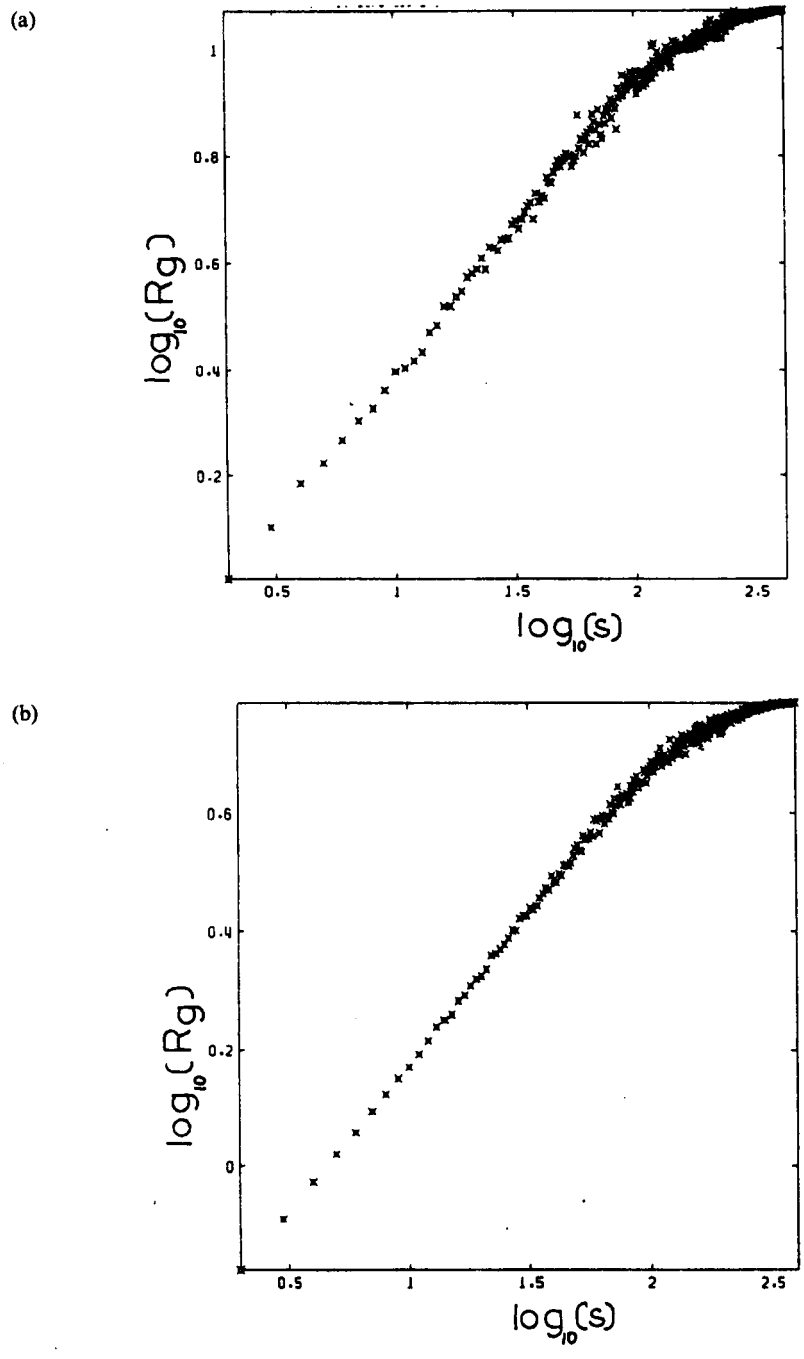

Figure 5 The s-dependence of the radius of gyration, R_g, for the LJ state points, (a) $p_c = 0.271699$ (×), $T = 10.0$, $\sigma_s = 2.0$, $2d$, $d_f = 1.77 \pm 0.1$ and $N = 450$; (b) $p_c = 1.010848$ (×), $T = 5.0$, $\sigma_s = 1.0$, $2d$, $d_f = 1.90 \pm 0.1$ and $N = 450$.

(c)

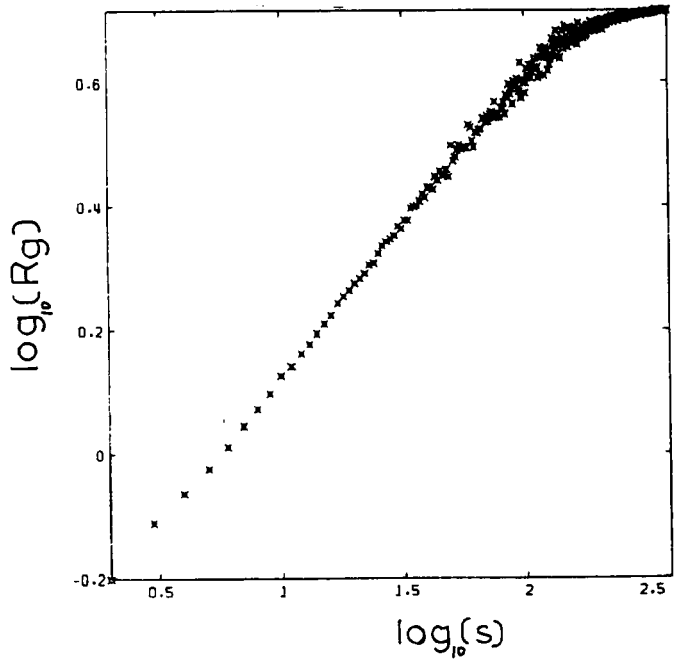

(d)

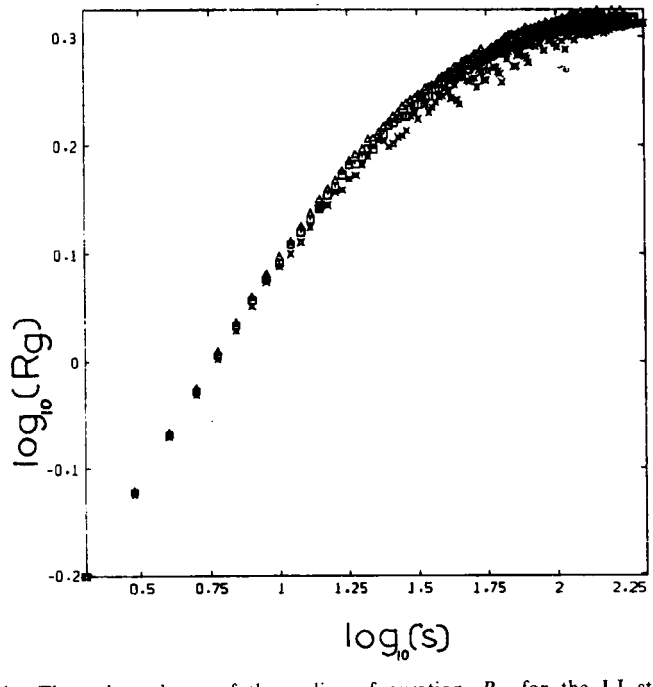

Figure 5 (*continued*) The s-dependence of the radius of gyration, R_g, for the LJ state points, (c) $p_c = 1.398381$ (×), $T = 0.6$, $\sigma_s = 0.9$, $2d$, $d_f = 2.0 \pm 0.1$ and $N = 450$; (d) $p_c = 1.2564$ (square), $p = 1.3125$, (×), $p = 1.204917$ (△) $T = 6.0$, $\sigma_s = 0.92226$, $3d$, $d_f = 2.36 \pm 0.1$ and $N = 256$.

becomes more positive, i.e., $n_s(p) \leq n_s(p_c)$. Figure 4(a), (b) and (c) for the $3d$ states reveal that these predictions are reproduced from the MD simulations.

We now look at the tenuity of the non-percolating clusters at the percolation threshold by considering their radius of gyration, R_g,[6],

$$R_g = \frac{1}{2} < \sum_{i}^{s-1} \sum_{j \neq i}^{s} R_{ij}^2 / s(s-1) >^{1/2}, \tag{19}$$

where $\underline{R}_{ij}$ is the vector separation between particles i and j. The scaling relationship here is $R_g \propto s^{1/d_f}$ as $s \to \infty$. Figure 5 gives typical examples for $2d$ and $3d$ supercritical fluid LJ states about the percolation threshold. There is an intermediate s regime where this scaling relationship is obeyed. In $2d$ we obtain $d_f = 1.90 \pm 0.05$, in excellent agreement with the accepted value for $2d$ static random percolation, $D_f = 1.9$[6]. In $3d$ we obtain $d_f = 2.35 \pm 0.10$, slightly lower than the accepted value for $3d$ static random percolation, $D_f = 2.5$[6]. In practice, this scaling relationship applies well for $0.2 \leq P \leq 0.8$. Therefore the fractal dimension of the percolating clusters is insensitive to p about p_c. As exhibited by n_s, the finite size of the MD cell leads to deviations from scaling laws in the $s \to N$ limit.

The characteristic lengthscale, ξ, is defined by.

$$\xi^2 = \frac{\sum_s s^2 n_s R_g^2}{\sum_s s^2 n_s}. \tag{20}$$

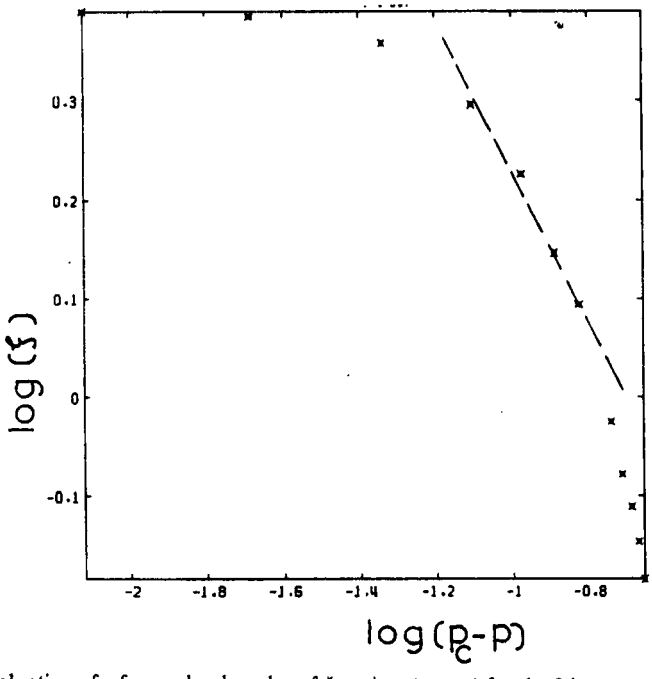

Figure 6 Evaluation of ν from a log-log plot of ξ against $(p_c - p)$ for the $3d$ state: $T = 6.0$, $\sigma_s = 1.31751$, $p_c = 0.26262$, $N = 108$. The states for $p < p_c$ are considered. The superposed line has a slope $(= -\nu)$ of 0.8 ± 0.1.

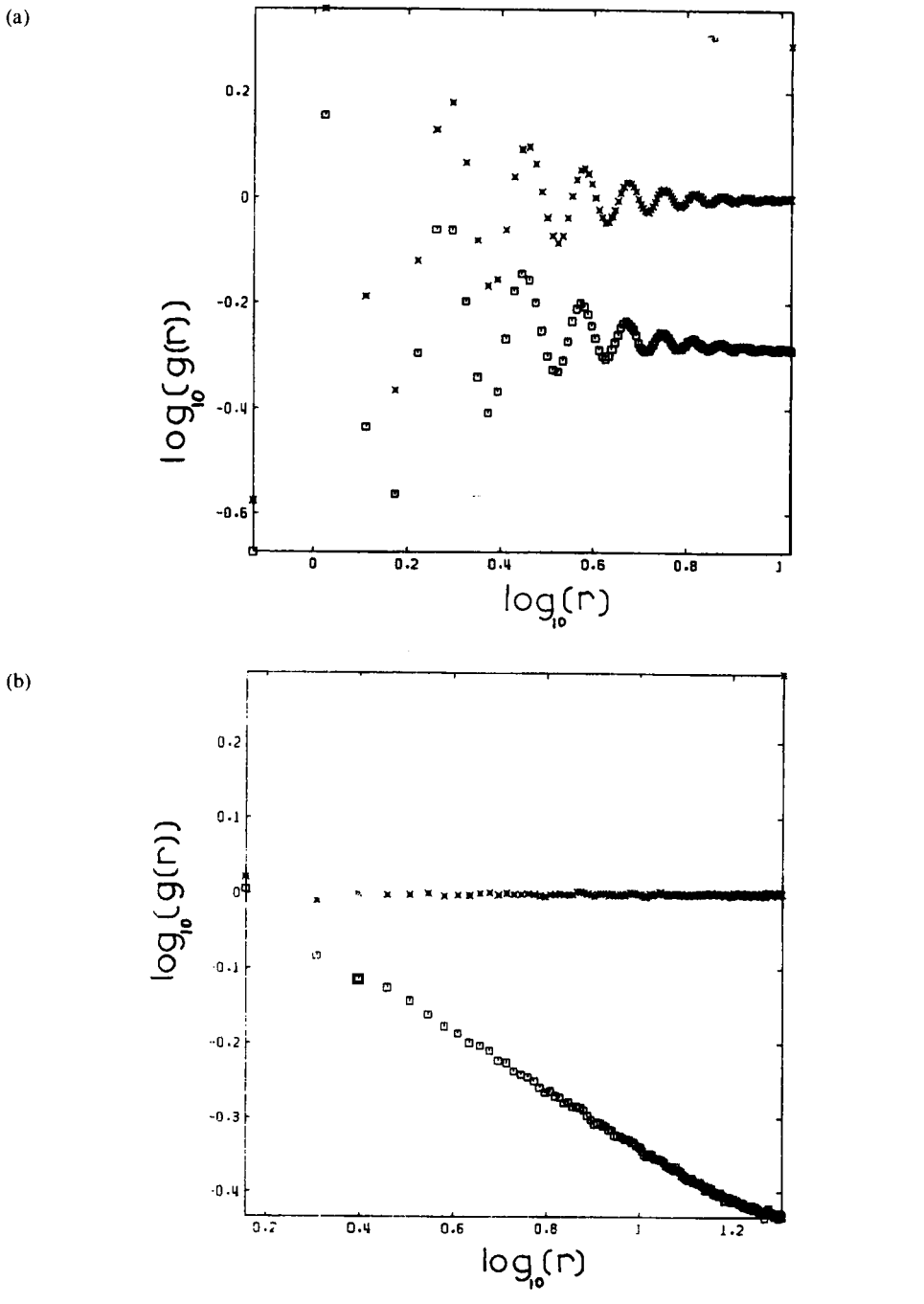

Figure 7 Log-log plot of $g(r)$, (×), and $p(r)$, (square), for the following $2d$ states: (a) $p_c = 1.010848$, $T = 5.0$, $N = 450$, $\sigma_s = 1.0$ and (b) $p_c = 0.271699$, $T = 10.0$, $N = 450$, $\sigma_s = 2.0$ where $d_f = 1.6 \pm 0.2$ from the linear part of $p(r)$.

Use of Eqns. (2) and (20) leads to ν. Note that this is an alternative route to ν, supplementing that from the percolation fraction. In Figure 6 we present a typical plot of $\log \xi$ against $\log(p - p_c)$ for $3d$ LJ fluids. For $(p - p_c) \to 0$ the ξ curve is distorted by the finite-N value. As $(p - p_c) \to \infty$ there is a distortion due to the limitation on the smallness of the cluster (i.e., 1 LJ atom). Therefore the intermediate $(p - p_c)$ regime is likely to produce the most reliable estimate of ν from (1). For the states considered we obtain a value of $\nu = 0.8 \pm 0.1$ close to the random lattice value.

The pair radial distribution function, $g(r)$ and pair connectedness function, $p(r)$, for pair separations, r, are probes of the local structure in the whole fluid and in the percolating clusters, respectively[6,14]. They are formally very similar. In $3d$,

$$g(r) = n(r)/(4\pi r^2 \rho \delta r), \tag{21}$$

where δr is the radial increment for $n(r)$; $n(r)$ is the number of particles found on average within $r - \delta r/2 \leq r \leq r + \delta r/2$,

$$p(r) = n(r)P_\infty/(4\pi r^2 \rho \delta r). \tag{22}$$

The search for pairs in $p(r)$ is restricted to those particles within the same PC. As $r \to \infty$ then $p(r) \to P_\infty^2$. For finite r there is a regime in which $p(r) \sim r^{d_f - d}$. For the small N considered here it is not possible to go out far enough in r to determine D_f in the hard-core limit. The $p(r)$ look similar to the $g(r)$ but attain a lower limiting value. When the pair separation becomes comparable to L the dimension of PC must approach the dimension of the space, d ($=3$ here). This is a finite-size artefact. In the hard-core limit the $p(r)$ shows many oscillations similar to $g(r)$ up to $r \approx L/2$. Therefore the finite size of the cell precludes us from observing long-range correlations of the particles, especially for $d = 2$ where d_f is very close to d. There is not sufficient r range to extract a d_f. The low-density soft-core limit has fewer oscillation for the short range structure. Also a greater range of distance can be covered for a fixed N. The $g(r)$ and $p(r)$ for two $2d$ LJ states are given in Figure 7. The high density state in Figure 7(a) is at $p_c = 1.0108$ and $T = 5.0$, $\sigma_s = 1.0$. The d_f cannot be discerned from the oscillations. The Figure 7(b) examines a low density soft-core state in $2d$, clearly showing a linear regime in $p(r)$ symptomatic of a $D_f = 1.6 \pm 0.1$ below the Euclidean dimension.

The coordination number is straightforwardly defined on a lattice, but not for a continuum fluid. The coordination number for a continuum fluid is defined as the *average* number of molecules within σ_s about an arbitrary molecule. It changes dramatically with distance close to σ_s as it increases $\sim r^d$. This can be resolved into two components, the average obtained from all particles and their neighbours, n_1, determined from $g(r)$. There is also a coordination number, n_2, obtained only from the neighbours within the PC, coming from $p(r)$. In $2d$ n_1 decreases from *ca.* 6 to 2.5 on going from the hard-core to the soft-core limit. It increases somewhat as $T \to T_c$. The other co-ordination number n_2 is very close to the value of n_1 at each state point.

In both $2d$ and $3d$ n_2 must be greater than 2 (each particle must contain at least two neighbours to form a contiguous chain). In the soft-core limit the percolating cluster is mainly backbone (i.e., dangling branches do not dominate).

4 CONCLUSIONS

Until recently we did not have mathematical "tools" with which to characterise random aggregates that result from growth processes and appear in equilibrium fluid phases. The advent of percolation theory and fractals has changed this situation. We are now at the beginning of what is likely to be a rich field of research with many applications in the physical sciences.

Acknowledgements

D.M.H. gratefully thanks *The Royal Society* for the award of a *Royal Society 1983 University Research Fellowship*. He thanks J. R. Melrose for invaluable discussions.

References

1. B. B. Mandelbrot, *Les Objets Fractal: Forme, Hasard et Dimension* (Flamarion, Paris, 1975).
2. R. Jullien, *Contemp. Phys.*, **28**, 477-493 (1987).
3. E. Guyon, in *Les Houches, Session XLVI-Le Hasar et la matiere*, (Elsevier, 1987), ed. J. Souletie, J. Vannimenus and R. Stora, pp. 71-156.
4. D. W. Schaefer, J. E. Martin, P. Wiltzius and D. S. Cannell, *Phys. Rev. Lett.* **52**, 2371 (1984).
5. P. N. Pusey and J. G. Rarity, *Mol. Phys.* **62**, 411-418 (1987).
6. H. J. Herremann, *Phys. Rep.* **136**, 153-227 (1986).
7. M. Matsushita, F. Family and K. Honda, *Phys. Rev. A*, **36**, 3518 (1987).
8. G. Bolle, C. Cametti, P. Codastefano and P. Tartaglia, *Phys. Rev. A* **35**, 837-841 (1987).
9. P. R. Sperry, *J. Coll. and Interface Sci.*, **99**, 97-108 (1984).
10. D. A. Weitz and J. S. Huang in *Kinetics of Aggregation and Gelation*, ed. F. Family and D. P. Landau, (Elsevier, 1984).
11. J. E. Martin, *Phys. Rev. A*, **36**, 3415-3426 (1987).
12. M. Adam, M. Delsanti, J. P. Munch and D. Durand, *Phys. Rev. Lett.* **61**, 706 (1988).
13. D. Stauffer, *Phys. Rep.* **54**, 1-74 (1979).
14. D. Stauffer, *Introduction to Percolation Theory* (Taylor and Francis, 1985, Chichester).
15. N. A. Seaton and E. D. Glandt, *J. Phys. A*, **20**, 3029 (1987).
16. L. C. Allen, B. Golding and W. H. Haemmerle, *Phys. Rev. B*, **37**, 3710-3712 (1988).
17. R. Buscall, P. D. A. Mills, J. W. Goodwin and D. W. Lawson, *J. Chem. Soc. Faraday Trans. I*, **84**, in press. (1988).
18. J. G. Zabolitzky, D. J. Bergman and D. Stauffer, *J. Stat. Phys.*, **44**, 211-223 (1986)
19. S. Feng, M. F. Thorpe and E. Garboczi, *Phys. Rev. B*, **31**, 276-280 (1985).
20. W. Tang and M. F. Thorpe, *Phys. Rev. B*, **35**, 5539-5551 (1988).
21. P. D. Beale and D. J. Srolovitz. *Phys. Rev. B*, **37**, 5500-5507 (1988).
22. E. T. Gawlinski and H. E. Stanley, *J. Phys. A: Math. Gen.*, **14**, L291 (1981).
23. I. Balberg and N. Binenbaum *Phys. Rev. A*, **31**, 1222 (1985).
24. I. Balberg and N. Binenbaum, *Phys. Rev. A*, **35**, 5174 (1987).
25. A. L. R. Bug, S. A. Safran, G. S. Grest, and I. Webman, *Phys. Rev. Lett.*, **55**, 1896 (1985).
26. N. A. Seaton and E. D. Glandt, *J. Chem. Phys.*, **86**, 4668 (1987).
27. A. Geiger and H. E. Stanley, *Phys. Rev. Lett.* **49**, 1895 (1982).
28. I. Balberg, *Phys. Rev. B*, **37**, 2391 (1988).
29. J. P. Lu and J. L. Birman, *J. Stat. Phys.*, **46**, 1057 (1987).
30. D. M. Heyes and J. R. Melrose, 1988, *Mol. Sim.* in press.
31. D. MacGowan and D. H. Heyes 1988, *Mol. Sim.*, **1**, 277 (1988).
32. K. D. Hammonds and D. M. Heyes, *J. Chem. Soc., Faraday Trans. II*, **84**, 705 (1988).
33. D. M. Heyes and J. R. Melrose, *J. Phys. A*, 1988, in press.